

Pseudo-spin model of argentophilicity in honeycomb bilayered materials

Godwill Mbiti Kanyolo^{1, 2, *} and Titus Masese^{1, 3, †}

¹Research Institute of Electrochemical Energy (RIECEN),

National Institute of Advanced Industrial Science and Technology (AIST),

1-8-31 Midorigaoka, Ikeda, Osaka 563-8577, Japan

²The University of Electro-Communications, Department of Engineering Science,

1-5-1 Chofugaoka, Chofu, Tokyo 182-8585, Japan

³AIST-Kyoto University Chemical Energy Materials Open Innovation Laboratory (ChEM-OIL),
Yoshidahonmachi, Sakyo-ku, Kyoto-shi 606-8501, Japan

We introduce a pseudo-spin model of the argentophilic bond expected in silver-based bilayered materials arising from a spontaneous pseudo-magnetic field interacting with pseudo-spins of two unconventional Ag ions, namely Ag^{2+} and Ag^{1-} electronically distinct from (albeit energetically degenerate to) the conventional Ag^{1+} cation typically observed in monolayered materials. This model suggests the possibility of tuning the dimensionality and hence the conductor-semiconductor-insulator properties of honeycomb layered materials by application of external electric and magnetic fields, analogous to driving a superconducting system to the normal regime by critical electric and magnetic fields.

Introduction.—Due to energy proximity of silver $4d^{10}$ and $5s^1$ electrons and environmental factors in silver-based honeycomb bilayered materials such as crystal field splitting of the $4d$ orbitals encouraging sd hybridisation, the electronic configuration of silver atom (Ag) can be in either one of two degenerate states, namely the expected $[\text{Kr}]4d^{10}5s^1$ configuration responsible for the oxidation state Ag^{1+} or the proposed $[\text{Kr}]4d^95s^2$ configuration.[1] This suggests two other oxidation states exist, namely Ag^{2+} and Ag^{1-} , obtained by designating the electrons in either the $5s^2$ or $4d^9$ orbitals respectively as the valence electrons (or both, in the case of Ag^{3+}). While these degenerate states have been found to exist independently in various materials such as the anti-ferromagnetic material $\text{Ag}^{2+}\text{F}_2^{1-}$ and silver clusters Ag_N^{1-} ($N = 1$)[2–7], by a theorem analogous to Peierls[8–10], their co-existence requires their energy degeneracy to be spontaneously broken for the material to ultimately achieve stability.[1, 11, 12]

For exemplar silver-based bilayered materials not limited to $\text{Ag}_6^{1/2+}\text{M}_2\text{TeO}_6$ ($\text{M} = \text{Ni, Co, Mg, Cu etc}$) whose structure is shown in Figure 1, it has been proposed that the coexistence of the silver degenerate states naturally results in anomalous valence states (subvalent states) such as $\text{Ag}_2^{1/2+} = \text{Ag}^{2+}\text{Ag}^{1-}$ or $\text{Ag}_3^{2/3+} = \text{Ag}^{2+}\text{Ag}^{1-}\text{Ag}^{1+}$, which also requires the dimerisation of the two silver atoms in each primitive cell of the bipartite honeycomb lattice, enabled by argentophilicity.[1] It is this dimerisation that we propose to be the manifestation of pseudo-spin interactions with pseudo-magnetic fields in silver-based bilayered materials. In silver metal, pseudo-spin as the explanation for argentophilicity is superfluous since the concept of metallic bonds already suffices. Particularly, metallic bonds arise whenever the valence electrons are extremely delocalised, leading to their collective sharing amongst the metallic ions. Meanwhile, the argentophilic bonds in silver bilayers are not

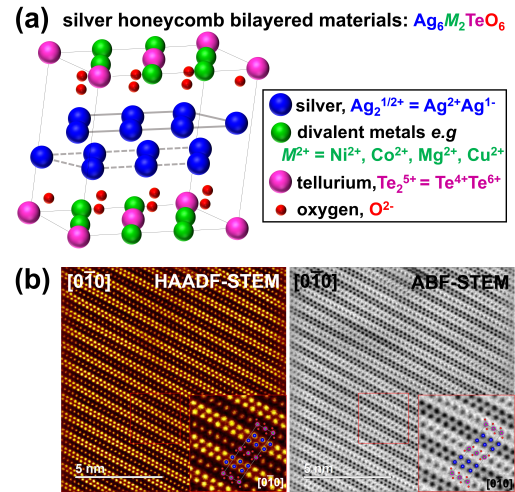


FIG. 1. Crystalline structure of the recently discovered silver-based honeycomb bilayered material $\text{Ag}_6^{1/2+}\text{M}_2\text{TeO}_6$ where in a) the valence $1/2+$ silver cations ($\text{Ag}_2^{1/2+} = \text{Ag}^{2+}\text{Ag}^{1-}$) are shown in blue, the divalent metal cations ($\text{M}^{2+} = \text{Ni}^{2+}, \text{Co}^{2+}, \text{Mg}^{2+}, \text{Cu}^{2+}$ etc) are shown in green, tellurium cations $\text{Te}_2^{5+} = \text{Te}^{4+}\text{Te}^{6+}$ are shown in magenta and oxygen anions (O^{2-}) are shown in red. (b) Crystalline structure of $\text{Ag}_6\text{Ni}_2\text{TeO}_6$ obtained from the $[010]$ direction by the high-angle annular dark-field (HAADF) and annular bright-field (ABF) scanning transmission electron microscope (STEM) techniques clearly showing the silver bilayers (inset).[1]

only shorter than silver metallic bonds ($\leq 2.83 \text{ \AA}$ and $\leq 2.89 \text{ \AA}$ in bilayered silver structures and elemental silver respectively)[1], but also require the valence electrons to be localised. This has led some researchers to consider electron localisation schemes in order to augment this discrepancy with the metallic bond picture.[13–15]

In the scheme involving silver degenerate states[1], localisation of silver valence electrons is already im-

plied by the involvement of the electronic configuration $[\text{Kr}]4d^95s^2$ (particularly, $4d_{z^2}5s^2$) obtained by *sd* hybridisation instead of the conventional $4d^{10}5s^1$ electronic configuration with the usually itinerant $5s^1$ valence electrons localised by the closed-shell pairing in $5s^2$ state. In addition, like in graphene, the pseudo-spins on the bipartite honeycomb lattice are inherited from the behaviour of actual spins of the $4d_{z^2}^1$ orbital electrons[12, 16–19] *albeit* the pseudo-spin degree of freedom in silver is expected to clearly manifest for an isolated $4d_{z^2}^1$ orbital due to $4d^9$ crystal field splitting in linear or prismatic coordination to anions such as F^{1-} or O^{2-} .[1]

Herein, it is prudent to employ units where reduced Planck's constant and speed of mass-less particles in the material are set to unity ($\hbar = \bar{c} = 1$).

Pseudo-spin model.—Consider *sd* hybridisation as the interaction between localised spin impurities S_α^z and S_β^z ($\alpha, \beta = i, j, k$) on a honeycomb lattice comprising isolated $4d_z^1$ orbitals in the Ag configuration, $[\text{Kr}]4d^95s^2$, mediated by conduction electrons comprising the $5s^2$ orbitals as illustrated in Figure 2. This leads to the exchange interaction terms $J(\vec{r}_{ij})$ between i and j atoms and possible linear terms $h(\vec{r}_{ij})$ in the Heisenberg Hamiltonian[10, 20],

$$H = \sum_{i,j \in hc \in R^d \setminus i=j} [f(\vec{r}_{ij}) + 4J(\vec{r}_{ij}) (\langle S_i^z S_j^z \rangle + 1/4)] \\ = \sum_{i,j \in hc \in R^d \setminus i=j} [4J(\vec{r}_{ij}) \langle S_i^z S_j^z \rangle + h(\vec{r}_{ij}) \langle (S_i^z + S_j^z) \rangle], \quad (1a)$$

under the constraint,

$$f(\vec{r}_{ij}) = -J(\vec{r}_{ij}) + h(\vec{r}_{ij}) \langle (S_i^z + S_j^z) \rangle, \quad (1b)$$

where the sum is evaluated over silver atoms i and j excluding $i \neq j$ in a potentially bifurcated bipartite honeycomb hexagonal lattice (hc) comprising a pair of hexagonal lattices (hx, hx^*) displaced along the z direction in Euclidean space R^d (bifurcated honeycomb lattice) when $d = 3$ dimensions (3D), and non-bifurcated for $d = 2$ dimensions (2D) in the plane, R^2 , as displayed in Figure 3. Here, $f(\vec{r}_{ij})$, $J(\vec{r}_{ij})$ and $h(\vec{r}_{ij})$ are yet unknown energy functions of the relative positions $\vec{r}_{ij} = \vec{r}_i - \vec{r}_j$ of next neighbour Ag atoms i, j at positions \vec{r}_i and \vec{r}_j respectively, and S_i^z or S_j^z are the z direction spin operators for pseudo-spin impurities at i, j ($4d_{z^2}^1$ electron spins in each $4d^95s^2$ Ag atom) within a sea of conduction electrons. In this picture, the bond length is given by the silver separation distance, $r_{ij} = |\vec{r}_{ij}| \equiv r_{\text{bond}}$ when $H = 0$. Thus, figuring out the functional form of the unknown energy functions on the honeycomb lattice which satisfy $H = 0$ either analytically or via *ab initio* calculations amounts to solving the bifurcation problem, whose results can then be compared with experiment. In this endeavour, next-neighbour summation approximation may be taken

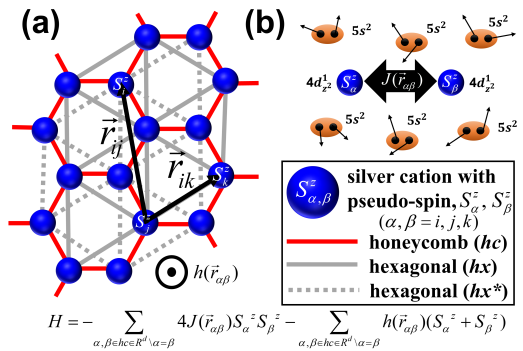


FIG. 2. Pseudo-spin model introduced on the bipartite $\text{Ag}_2^{1/2+} = \text{Ag}^{2+}\text{Ag}^{1-}$ honeycomb lattice (hc) consisting of a pair of equivalent hexagonal lattices (hx and hx^*). (a) Vectors $\vec{r}_{ij} \in R^d$ ($d = 2, 3$) and $\vec{r}_{ik} \in R^2$ depicted on the honeycomb lattice spanning between the centres of Ag cations i and j (blue) with pseudo-spins S_i^z and S_j^z respectively, and Ag cations i and k with pseudo-spins S_i^z and S_k^z respectively. The pseudo-spins can interact with a pseudo-magnetic field $h(\vec{r}_{\alpha\beta})$ ($\alpha, \beta = i, j, k$) along the z direction. (b) A depiction of the exchange coupling, $J(\vec{r}_{\alpha\beta})$ between two $4d_{z^2}^1$ magnetic impurities introduced by Ag^{2+} cations at α and β with pseudo-spins S_α^z and S_β^z , mediated by a sea of itinerant $5s^2$ electrons of $\text{Ag}^{1-} = \text{Ag}^{1+} + 2e^-$. The total interaction, H excluding terms with $\alpha = \beta$ corresponds to eq. (1).

provided it is justified on physical grounds. While particularly unwieldy, similar computational challenges have been overcome for the analogous problem in $d = 1$ dimensions (1D), corresponding to the case of dimerisation of carbon atoms in polyacetylene and other similar conjugated hydrocarbons.[10, 20]

Nonetheless, we are solely interested in pursuing the analytic behaviour of eq. (1), starting with the simplest case of the two-body problem. The next-neighbour pseudo-magnetisation and pseudo-spin correlation expectation values are given by,

$$\tilde{m}^z = \langle (S_i^z + S_j^z) \rangle = 0, \pm 1, \quad (2a)$$

$$\tilde{c}^z = \langle S_i^z S_j^z \rangle = -1/4, +3/4, \quad (2b)$$

respectively, which can be associated with the pseudo-spin wave functions as follows,

wave function, Σ_{ij}	magnetisation	correlation
$\frac{1}{\sqrt{2}} (\uparrow\downarrow \rangle - \downarrow\uparrow \rangle)$,	$\tilde{m}^z = 0$,	$\tilde{c}^z = -1/4$,
$\frac{1}{\sqrt{2}} (\uparrow\downarrow \rangle + \downarrow\uparrow \rangle)$,	$\tilde{m}^z = 0$,	$\tilde{c}^z = +3/4$,
$ \uparrow\uparrow\rangle$,	$\tilde{m}^z = 1$,	$\tilde{c}^z = +3/4$,
$ \downarrow\downarrow\rangle$,	$\tilde{m}^z = -1$,	$\tilde{c}^z = +3/4$.

It is prudent to also consider the actual spin magnetisation and correlations in the z direction given by,

$$m^z = \langle (s_i^z + s_j^z) \rangle = 0, \pm 1, \quad (3a)$$

$$c^z = \langle s_i^z s_j^z \rangle = -1/4, +3/4, \quad (3b)$$

respectively where s_i, s_j are the actual spin operators, which can be associated with the actual spin wave functions as follows,

wave function, σ_{ij}	magnetisation	correlation
$\frac{1}{\sqrt{2}} (u d\rangle - d u\rangle)$,	$m^z = 0$,	$c^z = -1/4$,
$\frac{1}{\sqrt{2}} (u d\rangle + d u\rangle)$,	$m^z = 0$,	$c^z = +3/4$,
$ u u\rangle$,	$m^z = 1$,	$c^z = +3/4$,
$ d d\rangle$,	$m^z = -1$,	$c^z = +3/4$.

Here, $|u\rangle$ and $|d\rangle$ are respectively the spin up and down wave functions of itinerant $5s^2$ silver conduction electrons, to be distinguished from the pseudo-spin up and down wave functions, $|\uparrow\rangle$ and $|\downarrow\rangle$ respectively considered to originate from the spins of localised $4d_{z^2}^1$ silver electrons. Thus, using the notation, $\Sigma_{ij} = (\tilde{m}^z, \tilde{c}^z)_{ij}$ to label the pseudo-spin wave functions and $\sigma_{ij} = (m^z, c^z)_{ij}$ to label the actual spin wave functions, we can consider the parity of the spatial wave functions in order to extract valuable information about the ground state of the pseudo-spin system given by eq. (1).

In particular, the spatial two-particle wave function $\psi_{\pm}(\vec{r}_{ij})$ of adjacent silver fermions in the absence of pseudo-spin degrees of freedom must satisfy,

$$\begin{aligned} \psi_{\pm}(\vec{r}_{ij})\sigma_{ij}^{\mp} &= -\psi_{\pm}(\vec{r}_{ji})\sigma_{ji}^{\mp} \\ &= \frac{1}{2} [\phi_i(\vec{r}_i)\phi_j(\vec{r}_j) \pm \phi_i(\vec{r}_j)\phi_j(\vec{r}_i)] \sigma_{ij}^{\mp}, \end{aligned} \quad (4)$$

implying $\sigma_{ij}^{\mp} = \mp\sigma_{ji}^{\mp}$, where $\phi_i(\vec{r}), \phi_j(\vec{r})$ is the spatial wave function of a conduction electron at \vec{r}_i, \vec{r}_j hopping between Ag cations on adjacent lattice sites and $\vec{r}_{ij} = \vec{r}_i - \vec{r}_j$. However, assuming the honeycomb lattice introduces the pseudo-spin degree of freedom with wave functions, Σ_{ij} the composite two-silver wave function can be written in a generic form as,

$$\begin{aligned} \psi^p(\vec{r}_{ij})\Sigma_{ij}^a\sigma_{ij}^b &= -\psi^p(\vec{r}_{ji})\Sigma_{ji}^a\sigma_{ji}^b \\ &= \frac{1}{2} [\phi_i(\vec{r}_i)\phi_j(\vec{r}_j) + p\phi_i(\vec{r}_j)\phi_j(\vec{r}_i)] \Sigma_{ij}^a\sigma_{ij}^b, \end{aligned} \quad (5)$$

where $p = \pm$, $a = \pm$ and $b = \pm$ indicate the symmetry (+)/anti-symmetry (-) of the respective wave functions. For instance, for plane wave solutions, the symmetry/anti-symmetry of the spatial wave function corresponds to even/odd parity. This is evident for a model comprising left- and right-moving plane waves of conduction electrons hopping between Ag^{2+} and Ag^{1-} along a honeycomb edge,

$$\phi_i(\vec{r}_i) = \frac{1}{\sqrt{\Omega}} \exp(\# \sqrt{-1} \vec{k}_F \cdot \vec{r}_i), \quad (6a)$$

$$\phi_j(\vec{r}_j) = \frac{1}{\sqrt{\Omega}} \exp(\# \sqrt{-1} \vec{k}_F \cdot \vec{r}_j), \quad (6b)$$

where \vec{k}_F is the Fermi wave vector and their chirality is given by $\# = \pm$, where Ω is the wave function normalisation factor. Requiring next-neighbour interacting Ag

states to have opposite chirality inherited from the conduction electrons (a requirement for the generation of a mass term between Ag^{2+} and Ag^{1-} [1]), we obtain plane wave solutions of the spatial wave function,

$$\phi^p(\vec{r}_{ij}) = \begin{cases} \Omega^{-1} \cos(\vec{k}_F \cdot \vec{r}_{ij}), & p = +, \\ \Omega^{-1} \sqrt{-1} \sin(\vec{k}_F \cdot \vec{r}_{ij}), & p = -, \end{cases} \quad (7)$$

appearing in eq. (4).

Proceeding, the only possible signs for a pair of silver fermions are given by the following cases:

cases :		
<i>p</i>	<i>a</i>	<i>b</i>
1.	+	+
2.	+	-
3.	-	-
4.	-	+

Moreover, assuming potentials $h(\vec{r}_{ij})$ and $J(\vec{r}_{ij})$ are symmetric in \vec{r}_{ij} and the Hamiltonian H commutes with the parity operator, the odd parity states ($p = -$) in eq. (8) are forbidden by a known theorem that the ground state is even parity.[21] Thus, we should cross out all the $p = -$ states, which leaves the only viable ground state as,

ground states :		
<i>p</i>	<i>a</i>	<i>b</i>
1.	+	-
2.	+	+

Note that, for vanishing respective magnetic fields, each of these ground states are 3-fold degenerate. However, degeneracy of the ground state is forbidden by a theorem by Peierls, which guarantees that the lattice must distort to lift the degeneracy.[8–10] Identifying the distortion on the honeycomb lattice with the finite pseudo-magnetic interaction, $h(\vec{r}_{ij}) \neq 0$, we find the unique ground state,

ground state :		
<i>p</i>	<i>a</i>	<i>b</i>
1.	+	-

where the pseudo-magnetic interaction (responsible for the bifurcation of the monolayered silver honeycomb lattice into bilayers[1]) must appear spontaneously thus breaking the degeneracy. On the other hand, a finite actual magnetic field selects instead the other ground state,

ground state :		
<i>p</i>	<i>a</i>	<i>b</i>
2.	+	+

which is guaranteed to be non-degenerate (by the presence of the magnetic field).

Consequently, due to the wave function symmetry considerations given in eq. (11), such a ground state must be without strain or distortions ($h(\vec{r}_{ij}) = 0$), implying a finite external magnetic field is present,

$$B \equiv (\vec{\nabla} \times \vec{A})_z \neq 0, \quad (12)$$

which tunes the argentophilic bond (\vec{A} is the electromagnetic vector potential) and hence the monolayer-bilayer phase transition, thus altering the dimensionality of the Ag lattice from 3D back to 2D, corresponding to the displayed lattices in Figure 3. Intuitively, the pseudo-magnetic interaction is analogous to the order parameter in the Ginzburg-Landau or the energy gap in Bardeen-Cooper-Schrieffer (BCS) theories of superconductivity, which are related and can be tuned by an external magnetic field driving the superconducting state to normal.[22]

Paired electrons.—The time component of the conduction electron wave functions $\phi_{i,j}(\vec{r}_{i,j})$ or the overall silver ground state wave function is the phase factors, $\exp(-iE_{\pm}t)$ where the dispersion relation at any honeycomb vertex with a Ag^{2+} or Ag^{1-} ion satisfies the linear dispersion relation, $E_{\pm} = \pm|\vec{k}_{\text{F}}|$ and \pm reflects the electron(+) / hole(−) energy dispersion relations. Thus, the Green's function of interest is the appropriately defined Fourier transform of the phase factor[23],

$$\begin{aligned} \mathcal{G}_{\pm}(\omega) &= \frac{1}{\omega - E_{\pm} + i\epsilon} \\ &= -i \int_{-\infty}^{\infty} dt \exp(i\omega t - \epsilon t) \theta(t) \exp(-iE_{\pm}t), \quad (13) \end{aligned}$$

where $i = \sqrt{-1}$, $\theta(t)$ is the Heaviside step function restricting the Fourier transform to the range $0 \leq t \leq \infty$ and $\epsilon \simeq 0$ is the infinitesimal with the properties $\epsilon \times \infty = \infty$ and $\epsilon \times 0 = 0$. In subsequent calculations using the Green's function, we shall set $\epsilon = 0$.

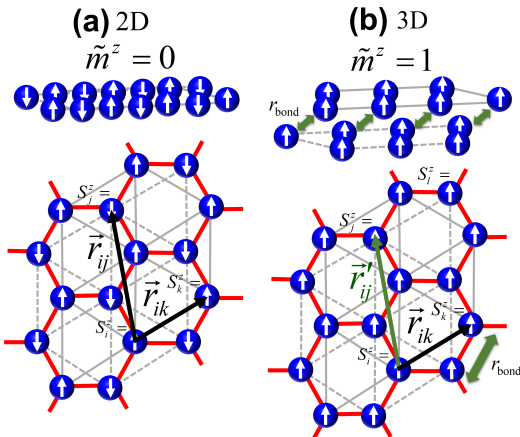


FIG. 3. Bipartite honeycomb lattice (2D) of silver cations (blue spheres) with pseudo-magnetisation $\tilde{m}^z = 0$ and its bifurcated counterpart (3D) with $\tilde{m}^z = 1$, where (a) and (b) depict the vectors and pseudo-spins in Figure 2. The vectors in black lack a z component ($\vec{r}_{ij}, \vec{r}_{ik} \in R^2$) whereas the z component of the vector in green is finite ($\vec{r}_{ij} \in R^3$) due to bifurcation, with r_{bond} and the green double arrow indicating the argentophilic bond.

Now, departing from only considering adjacent Ag ions in the two-body problem, but assuming that the adjacent pseudo-spins on the honeycomb lattice are *anti-parallel* as shown in Figure 3(a), the modification of the electron dispersion relation by interactions with the pseudo-magnetisation component of H in eq. (1) identically vanishes since,

$$\begin{aligned} U &= \sum_{i,j \in hc \in R^2 \setminus i=j} h(\vec{r}_{ij}) \langle (S_i^z + S_j^z) \rangle \\ &= \sum_{i,j \in hx \setminus i=j} h(\vec{r}_{ij}) \langle (S_i^z + S_j^z) \rangle + \sum_{i,j \in hx^* \setminus i=j} h(\vec{r}_{ij}) \langle (S_i^z + S_j^z) \rangle \\ &\quad + \sum_{i,j \in hc \in R^2 \setminus i=j, \vec{r}_{ij} \in hx, hx^*} h(\vec{r}_{ij}) \langle (S_i^z + S_j^z) \rangle \\ &= \sum_{i,j \in hx \setminus i=j} h(\vec{r}_{ij}) \times 1 + \sum_{i,j \in hx^* \setminus i=j} h(\vec{r}_{ij}) \times -1 \\ &\quad + \sum_{i,j \in hc \in R^2 \setminus i=j, \vec{r}_{ij} \in hx, hx^*} h(\vec{r}_{ij}) \times 0 = 0. \quad (14) \end{aligned}$$

On the other hand, considering adjacent pseudo-spins to be *parallel* instead (e.g. pseudo-spin *up* commensurate with the bifurcated lattice shown in Figure 3(b)), only the vectors not within the 2D hexagonal lattices $\vec{r}_{ij} \notin R^2$ (*i.e.* $i, j \in hc \in R^3 \setminus i \neq j, \vec{r}_{ij} \in R^2$) will have a finite z component,

$$\begin{aligned} U &= \sum_{i,j \in hc \in R^3 \setminus i=j} h(\vec{r}_{ij}) \langle (S_i^z + S_j^z) \rangle \\ &= \sum_{i,j \in hx, hx^* \in R^2 \setminus i=j} h(\vec{r}_{ij}) \times 1 \\ &\quad + \sum_{i,j \in hc \in R^3 \setminus i \neq j, \vec{r}_{ij} \in R^2} h(\vec{r}_{ij}) \times 1 \\ &= U_{R^2} + U_{R^3}. \quad (15) \end{aligned}$$

Due to the finite z component, the second sum of terms given by U_{R^3} in eq. (15) together with the sum involving the functions $J(\vec{r}_{ij})$ in eq. (1) lead to the expression given in eq. (41a) for the argentophilic bond. Meanwhile, the first sum of terms in eq. (15) given by U_{R^2} leads to a mass gap for 2D electron (silver) dynamics on the bifurcated lattice.

To see this, we shall assume $|U_{R^2}|$ takes the same functional form in position as well as momentum space, which we can justify using eq. (22). Intuitively, this arises from the fact that the reciprocal of the hexagonal lattice is another hexagonal *albeit* with unit vectors rotated by $\pi/2$ and appropriately re-scaled momentum vectors. Now, we wish to calculate the effective Green's function due to interactions of $\mathcal{G}_+(\omega)$, $\mathcal{G}_-(\omega)$ and U_{R^2} given by,

$$\begin{aligned} \mathcal{G}_+^{\text{eff}}(\omega) &\equiv \mathcal{G}_+ + \mathcal{G}_+ U_{R^2} \mathcal{G}_- U_{R^2}^* \mathcal{G}_+ \\ &\quad + \mathcal{G}_+ U_{R^2} \mathcal{G}_- U_{R^2}^* \mathcal{G}_+ U_{R^2} \mathcal{G}_- U_{R^2}^* \mathcal{G}_+ + \dots \\ &= \frac{1}{\mathcal{G}_+^{-1} - |U_{R^2}|^2 \mathcal{G}_-} = \frac{\omega - E_-}{\omega^2 - E_{\pm}^2 - |U_{R^2}|^2}, \quad (16a) \end{aligned}$$

where we have used the generic expression $w(1 + z + z^2 + \dots) = 1/(w^{-1} - z)$ under a regularisation scheme for values of $|z| > 1$ where z, w can be arbitrary complex functions.[23] We can thus describe the electron (silver) interactions alongside their chiral degrees of freedom as four-spinors by a diagonalisation scheme into quasi-particle interactions of the form,

$$\begin{aligned} \mathcal{G}_+^{\text{eff}}(\omega) &= \frac{\omega - E_-}{\omega^2 + \mathcal{E}_- \mathcal{E}_+} = \frac{\mu_+^2}{\omega - \mathcal{E}_+} + \frac{\mu_-^2}{\omega - \mathcal{E}_-} \\ &= \frac{\mu_+^2}{\omega - \vec{k}_F \cdot \vec{\alpha} - |U_{R^2}| \gamma^0} + \frac{\mu_-^2}{\omega + \vec{k}_F \cdot \vec{\alpha} + |U_{R^2}| \gamma^0}, \end{aligned} \quad (16b)$$

amounting to the result obtained by a Bogoliubov transformation of the particle/quasi-particle fermionic (creation, annihilation) operators $(c^\dagger, c)/(d^\dagger, d)$ respectively[23] with $\mathcal{E}_\pm = \pm\sqrt{E_\pm^2 + |U_{R^2}|^2} = \pm(\vec{k}_F \cdot \vec{\alpha} + |U_{R^2}| \gamma^0)$ and,

$$\mu_\pm = \sqrt{\frac{1}{2} \left(1 \pm \frac{E_\pm}{\mathcal{E}_\pm} \right)}, \quad (17)$$

are the so-called BCS coherence factors in the Bogoliubov transformation,

$$d^\dagger = \mu_+ c^\dagger + \mu_- c, \quad (18)$$

$$d = \mu_+ c + \mu_- c^\dagger. \quad (19)$$

Note that, $c^2 = (c^\dagger)^2 = d^2 = (d^\dagger)^2 = 0$, $d^\dagger d + d d^\dagger = c^\dagger c + c c^\dagger = \mu_-^2 + \mu_+^2 = 1$, and γ^0 and $\vec{\alpha}$ are 4×4 matrices related to Dirac matrices $\gamma^\mu = \gamma^0(1, \vec{\alpha})$ which satisfy the Clifford algebra $\gamma_\mu \gamma_\nu + \gamma_\nu \gamma_\mu = 2\eta_{\mu\nu}$ with $\gamma_\mu = \eta_{\mu\nu} \gamma^\nu$ and $\eta_{\mu\nu}$ the Minkowski space-time metric tensor. Finally, it is clear that:

1. The Dirac mass corresponds to $m_{\Delta(d)} = |U_{R^2}|$ which must vanish at the critical point of the phase transition such as in eq. (14) even for $h(\vec{r}_{ij}) \neq 0$;
2. Moreover, from the conclusions using the parity argument above, U_{R^2} ought to depend on external magnetic fields tuning it in eq. (15) leading to $U_{R^2} = 0$;
3. This tuning is expected to be possible even when the bifurcated lattice has $g - 1$ vacancies extracted by external electric fields, where g is defined as the genus of an emergent manifold within the context of an idealised model[12, 24, 25];
4. The expression expected for the mass term is $m_{\Delta(d)} \equiv 2m\Delta(d)$, with m a constant with dimensions of mass/energy and $\Delta(d) = (d - 2)/2$ the conformal dimension for mass-less scalar fields.[1, 12]

Thus, determining an appropriate function $h(\vec{r}_{ij})$ in eq. (15) manifesting these properties, alongside $J(\vec{r}_{ij})$ is tantamount to finding a solution for the functional form of

the argentophilic bond in the bifurcated honeycomb lattice.

Proposed solution—Introducing the lattice constant a , the vectors in the hexagonal lattices satisfy $r_{ij}^2/a^2 = 2n$, where $n \in \mathbb{N}$ is a finite positive integer. Moreover, we shall consider a trial function for the pseudo-magnetic field,

$$h(\vec{r}_{ij}) = -\frac{m}{C} \left(\frac{\sqrt{2}a}{r_{ij}} \right)^{2(\hat{s} + \hat{s}^*)}, \quad (20)$$

consistent with an emergent Liouville conformal field theory (CFT)[12],

$$\begin{aligned} &-\frac{m}{C} \sum_{i,j \in hx, hx^* \in R^2 \setminus i=j} \exp(2(\hat{s} + \hat{s}^*)\Phi(\vec{r}_{ij})) \\ &= -\frac{m}{C} \sum_{i,j \in hx, hx^* \in R^2 \setminus i=j} \frac{(\sqrt{2}a)^{2(\hat{s} + \hat{s}^*)}}{r_{ij}^{2(\hat{s} + \hat{s}^*)}} \equiv U_{R^2}(\hat{s}, \hat{s}^*) \\ &= \sum_{i,j \in hx, hx^* \in R^2 \setminus i=j} h(\vec{r}_{ij}) = -\frac{2m}{C_{\text{eff}}} \sum_{n=1}^{\infty} \frac{C_n}{n^{\hat{s} + \hat{s}^*}}, \end{aligned} \quad (21)$$

with $1/C$ a proportionality constant, where $\Phi(\vec{r}_{ij}) = -\frac{1}{2} \ln(r_{ij}^2/(\sqrt{2}a)^2)$ is the Liouville field defined on the hexagonal lattices[12], the potential $U_{R^2}(\hat{s}, \hat{s}^*)$ is comprised solely of the sum over silver atoms i, j connected only by 2D vectors $\vec{r}_{ij} \in R^2$ in the hexagonal lattices i.e. $i, j \in hx, hx^* \in R^2$ $i = j$ (eq. (15)) with the lattice now assumed to extend to infinity in R^2 , \hat{s}, \hat{s}^* are scaling parameters to be solved for, which shall determine the mass term proportional to U_{R^2} and the coefficient C_n is the number of vectors of norm $2n$ on each hexagonal lattice. The effective proportionality constant $1/C_{\text{eff}} \propto 1/C$ arises from translating the sum over the silver atoms i, j to the sum over vectors $\vec{r}_{ij} \in hx, hx^* \in R^2$.

Notably, the coefficients C_n can be generated by the theta function of the hexagonal lattice,

$$\Theta_\Lambda(\tau) = \sum_{\vec{r}_{ij} \in \Lambda} \exp\left(i\pi\tau \frac{r_{ij}^2}{a^2}\right) = \sum_{n=0}^{\infty} C_n q^n(\tau), \quad (22a)$$

where $\Lambda = hx$ or hx^* , $q(\tau) = \exp(2\pi i\tau)$, $\tau \in \mathbb{H}_+$ is complex-valued and restricted to the upper-half plane, \mathbb{H}_+ and $r_{ij} = |\vec{r}_{ij}|$ is displayed in Figure 4. Thus, we can use the Poisson summation formula[12, 26] to yield the functional form of $\Theta_{\Lambda'}$ in momentum space ($\vec{k}_{ij} \in \Lambda'$),

$$\Theta_\Lambda(-1/\tau) = -i\tau\Theta_{\Lambda'}(\tau), \quad (22b)$$

$$\Theta_{\Lambda'}(\tau) = \sum_{\vec{k}_{ij} \in \Lambda'} \exp\left(i\pi\tau \frac{k_{ij}^2}{k_0^2}\right) = \sum_{n=0}^{\infty} C_n q^n(\tau), \quad (22c)$$

with $|\vec{k}_{ij}| = k_{ij}$, k_0 the lattice constant of Λ' satisfying $k_{ij}^2/2k_0^2 = n \in \mathbb{N}$ and $\vec{k}_{ij} \in \Lambda' =$

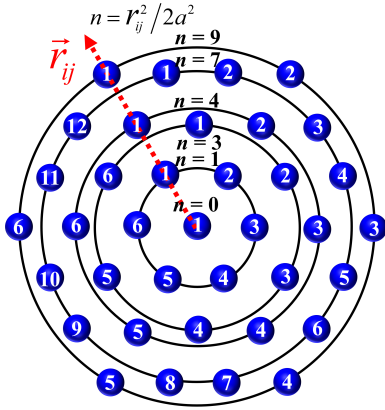


FIG. 4. Hexagonal lattice of Ag cations (blue) a distance $r_{ij} = a\sqrt{2n}$ radially apart from the origin ($n = 0$), where a is the lattice constant. The concentric black circles correspond to $n = 1, 3, 4, 7, 9 \dots$ with $n \rightarrow \infty$ assumed in calculations. The numbering in white is availed for ease of counting the number of vectors at a particular radial distance from the origin, displayed in eq. (23).

$\text{dual}(hx)$ or $\text{dual}(hx^*) = hx'$ or hx'^* . Thus, due to the same functional form between the lattice theta functions $\Theta_\Lambda(\tau)$ and $\Theta_{\Lambda'}(\tau)$, their Mellin transform under a change of variable $\tau = i\beta/2\pi$, is proportional to the potential U_{R^2} , taking the same functional form in position and momentum spaces.[12]

Proceeding, the summation in eq. (21) yields expressions where the first few coefficients are given by[27],

$$\frac{n}{C_n} \begin{array}{cccccccccc} 0 & 1 & 2 & 3 & 4 & 5 & 6 & 7 & 8 & 9 & \dots \\ \hline 1 & 6 & 0 & 6 & 6 & 0 & 0 & 12 & 0 & 6 & \dots \end{array} . \quad (23)$$

Nonetheless, we are interested in the continuum approximation, $C_n \rightarrow C_{n+1}$ and set $C_{\text{eff}} = C_n$ to yield,

$$U_{R^2}(\hat{s}, \hat{s}^*) \rightarrow -2m \sum_{n=1}^{\infty} \frac{1}{n^s} = -2m\zeta(s), \quad (24)$$

where $\zeta(s)$ is the Riemann zeta function and $s = \hat{s} + \hat{s}^*$. Famously, $\zeta(s)$ has an analytic continuation,

$$\zeta(s) = 2^s \pi^{s-1} \sin\left(\frac{\pi s}{2}\right) \Gamma(1-s) \zeta(1-s), \quad (25)$$

in the complex plane $s = \delta + i\gamma$ for real values of δ and γ , especially relevant in finding its values for $\delta < 1$ with,

$$\Gamma(s) = \int_0^\infty \frac{d\beta}{\beta} \beta^s \exp(-\beta), \quad (26)$$

the Gamma function. Thus, we find,

$$-\zeta(s) = \Delta(d) = \begin{cases} 0 & (s = -2g \neq 0) \\ 1/2 & (s = 0) \end{cases} , \quad (27)$$

where $\Delta(d) = (d-2)/2$, g is taken to be the genus of an emergent 2D manifold \mathcal{A}_g in the Liouville CFT and $-2g \neq 0$ are the so-called trivial zeros of $\zeta(s)$, as shown in Figure 5.

Transitions between these $g \in \mathbb{N}$ states labelling the number of vacancies $\nu = g-1 \geq 0$ or equivalently the genus of the emerging manifold \mathcal{A}_g with Gaussian curvature K satisfying,

$$2 - 2g = \frac{1}{2\pi} \int_{\mathcal{A}_g} d^2 r_{ij} K \exp(2\Phi(\vec{r}_{ij})), \quad (28)$$

can be induced by external electric fields,

$$\vec{E} \propto \vec{\nabla}\Phi = -K \exp(2\Phi), \quad (29)$$

which create or annihilate vacancies from the lattices should de-intercalation or intercalation processes in the bilayered material be electrochemically permitted.[12, 25, 28] One can thus conclude that the non-trivial solutions for $\zeta(s) = 0$ corresponding to mass-less particles on the honeycomb lattice should correspond to actual magnetic field terms applied to the bilayered material. The Riemann hypothesis[29] asserts that $s = 1/2 + i\gamma$, where our framework requires the so-called essential zeros at $\gamma = \gamma_g$ correspond to the flux values,

$$\gamma_g = \frac{1}{2\pi} \int_{\mathcal{A}_g} d^2 r_{ij} B(\vec{r}_{ij}), \quad (30)$$

due to the z component of the external magnetic field B given by eq. (12), where the mass term is modulated to vanish accordingly for $\gamma_g \neq 0$. The first three positive and negative values have been plotted in Figure 5.

To reflect these two pieces of actual and pseudo-magnetic information in a consistent mathematical framework, we propose a novel complex-valued tensor equation similar to the idealised model[24],

$$\partial_v K_{uv} = 4\pi\ell\Psi^* \partial_u \Psi, \quad (31a)$$

$$K_{uv} = \partial_u \partial_v \Phi - iq\epsilon_{uvw} A_w, \quad (31b)$$

where ℓ is a cut-off scale for electromagnetic interactions along the z direction, ∂_u are partial derivatives, $K_{uv} = K_{vu}^*$ is a complex-hermitian tensor, the repeated Euclidean indices u, v and w are summed over, $\Psi = \sqrt{\rho} \exp(iS)$, A_w , Φ , ϵ_{uvw} are the vacancy wave function, the electromagnetic vector potential, the Liouville field and the completely anti-symmetric Levi-Civita symbol respectively. One can check that, the vacancy number density in 3D is given by $\rho = -4\pi\ell K \exp(2\Phi)$ and S is the quantum phase.

Using this equation, we can introduce new complex

variables s, \bar{s} simply as,

$$\begin{aligned}
\hat{s} &= 2\ell \int_0^\ell \langle \Psi(z) | \partial_z | \Psi(z) \rangle_g dz \\
&= 2\ell \int_0^\ell \int_{\mathcal{A}_g} \Psi^*(\vec{r}_{ij}, z) \partial_z \Psi(\vec{r}_{ij}, z) d^2 r_{ij} dz \\
&= \ell \int_{\mathcal{A}_g} (|\Psi(\vec{r}_{ij}, \ell)|^2 - |\Psi(\vec{r}_{ij}, 0)|^2) d^2 r_{ij} \\
&+ i2\ell \int_0^\ell \int_{\mathcal{A}_g} \partial_z S(\vec{r}_{ij}, z) |\Psi(\vec{r}_{ij}, z)|^2 d^2 r_{ij} dz \\
&= -g + i\ell \langle \partial_z S \rangle_g = -g + i\gamma_g, \quad (32a)
\end{aligned}$$

and,

$$\begin{aligned}
\hat{s}^* &= 2\ell \int_0^\ell \langle \Psi^*(z) | \partial_z | \Psi^*(z) \rangle_g dz \\
&= 2\ell \int_0^\ell \int_{\mathcal{A}_g} \Psi(\vec{r}_{ij}, z) \partial_z \Psi^*(\vec{r}_{ij}, z) d^2 r_{ij} dz \\
&= \ell \int_{\mathcal{A}_g} (|\Psi(\vec{r}_{ij}, \ell)|^2 - |\Psi(\vec{r}_{ij}, 0)|^2) d^2 r_{ij} \\
&- i2\ell \int_0^\ell \int_{\mathcal{A}_g} \partial_z S(\vec{r}_{ij}, z) |\Psi(\vec{r}_{ij}, z)|^2 d^2 r_{ij} dz \\
&= -g - i\ell \langle \partial_z S \rangle_g = -g - i\gamma_g, \quad (32b)
\end{aligned}$$

where $\vec{r}_{ij} \in \mathbb{R}^2$ and we have defined $2\ell \int_{\mathcal{A}_g} |\Psi(\vec{r}_{ij}, 0)|^2 d^2 r_{ij} = 2(g - 1)$ for $g \neq 0$ and $2\ell \int_{\mathcal{A}_g} |\Psi(\vec{r}_{ij}, \ell)|^2 d^2 r_{ij} = -2$ corresponding to the negative values of the Euler characteristic, $-E(\mathcal{A}_g) = 2g - 2$ before ($g \neq 0$) and after ($g = 0$) bifurcation respectively, and $\langle \partial_z S \rangle_g = \int_0^\ell \int_{\mathcal{A}_g} \partial_z S(\vec{r}_{ij}, z) |\Psi(\vec{r}_{ij}, z)|^2 d^2 r_{ij}$.

Thus, from eq. (31), it is clear that a finite genus due to the external electric field in eq. (29) corresponds to the sum,

$$s = \hat{s} + \hat{s}^* = -2g, \quad (33)$$

whereas a finite magnetic flux due to the external magnetic field in eq. (30) corresponds to the imaginary part of \hat{s} or \hat{s}^* depending on the direction of B commensurate with eq. (27). Moreover, setting $S(\vec{r}_{ij}, z) + \Phi(\vec{r}_{ij}, z) = 0$ in eq. (32) guarantees flux is quantised $\gamma_g = g$, since there will be no distinctions between pseudo-magnetic and magnetic degrees of freedom,

$$|\Psi(\vec{r}_{ij}, z)|^2 = -K \exp(2\Phi(\vec{r}_{ij}, z))/4\pi\ell = \frac{B(\vec{r}_{ij})}{2\pi\ell}. \quad (34)$$

For instance, for 1D systems in a ring exhibiting Peierls instability, there are no distinctions between the pseudo-magnetic and actual magnetic degrees of freedom, which should lead to a magnetisation effect proportional to the order parameter[31]. However, we are interested instead in a different scenario where the actual magnetic and pseudo-magnetic effects are distinguishable, *i.e.*

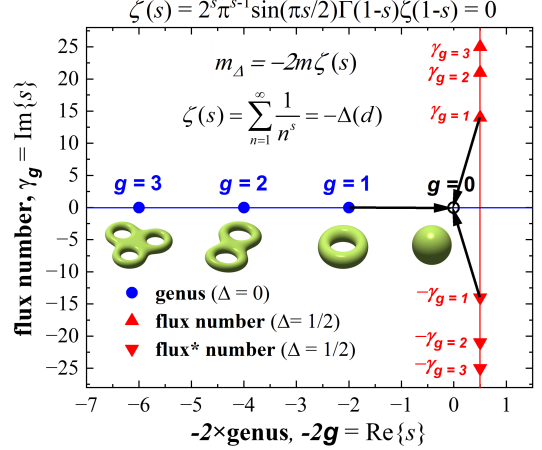


FIG. 5. Plot of genus versus magnetic flux numbers corresponding to a scale invariant $m_\Delta = 0$ theory on a bipartite lattice, suggested to be a good approximation for the case of the bifurcated bipartite honeycomb lattice in silver bilayered materials. Since the generated masses are proportional to the Riemann zeta function (eq. 24), this suggests scale invariant theories with $\zeta(s) = 0$, namely Liouville CFT and Chern-Simons theory (eq. (31)) on Riemannian manifolds \mathcal{A}_g shown in green with genus g , live at the trivial and essential zeros respectively, as depicted by the blue dots and red triangles. The essential zeros plotted were approximated to nearest integers[30], for ease of plotting. The triple point of the phase diagram at $g = 0$ (unshaded black dot) indicated by the black arrows corresponds to the condition for stable silver bilayers.

$S(\vec{r}_{ij}, z)$ and $\Phi(\vec{r}_{ij}, z)$ play complementary *albeit* antagonistic role in the realisation of a stable bilayered structure. An important scheme that implements this is to introduce quantum operators/averaging on $g = \nu - 1$ treated as quantum harmonic oscillator operators.[24] Setting $g = aa^\dagger$, $\nu = a^\dagger a$ where a^\dagger, a are the creation and annihilation operators satisfying the bosonic commutation relation $[a^\dagger, a] = 1$, we first take the quantum average of the genus via a weighted sum,

$$\langle g \rangle_{\mathcal{P}} = \sum_{\nu=0}^{\nu=\infty} g(\nu) \mathcal{P}_\nu(\beta) = \frac{1}{1 - \exp(-\beta)}, \quad (35a)$$

where $H_\nu = \nu + 1/2 = g - 1/2$ is the appropriately normalised Hamiltonian,

$$\mathcal{P}_\nu(\beta) = \frac{\exp(-\beta H_\nu)}{\sum_{\nu=0}^{\nu=\infty} \exp(-\beta H_\nu)}, \quad (35b)$$

is the probability for a certain genus to occur and β plays the role of the inverse temperature. Proceeding, using the gamma function, $\Gamma(\hat{s} = -2g)$ as a distribution function

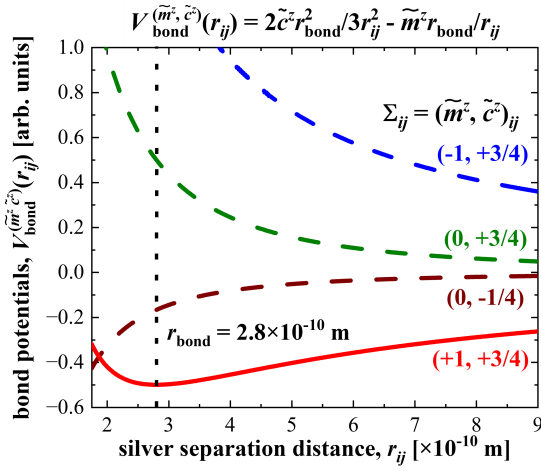


FIG. 6. Plot of the bond potentials $V_{\text{bond}}^{(\tilde{m}^z, \tilde{c}^z)}(r_{ij})$ appropriately defined in eq. (42), where \tilde{m}^z and \tilde{c}^z correspond to pseudo-magnetisation and correlation values of the wave functions Σ_{ij} in eq. (2c). It is clear that $\Sigma_{ij} = (+1, +3/4)$ represents the silver-silver bonding potential configuration with the argentophilic bond set at $r_{\text{bond}} = 2.8 \text{ \AA}$.

in a subsequent averaging[12] yields the result we seek,

$$\begin{aligned} \langle \langle g \rangle_{\mathcal{P}} \rangle_{\Gamma(-2g)} &= \frac{1}{\Gamma(-2g)} \int_0^\infty \frac{d\beta}{\beta} \beta^{-2g} \langle g \rangle_{\mathcal{P}} \exp(-\beta) \\ &= \frac{1}{\Gamma(-2g)} \int_0^\infty \frac{d\beta}{\beta} \beta^{-2g} \frac{1}{\exp(\beta) - 1} = \zeta(-2g), \end{aligned} \quad (35c)$$

subject to zeta function regularisation by eq. (25) for values $\text{Re}(s) = \delta < 1$. Evidently,

$$\tilde{s} = \langle \langle \hat{s} \rangle_{\mathcal{P}} \rangle_{\Gamma(-2g)} = \Delta(d) + i\gamma_g, \quad (36a)$$

$$\tilde{s}^* = \langle \langle \hat{s}^* \rangle_{\mathcal{P}} \rangle_{\Gamma(-2g)} = \Delta(d) - i\gamma_g, \quad (36b)$$

where the fluxes $\gamma_{g \neq 0} \neq 0$ must satisfy $\zeta(s) = 0$ in order to guarantee the vanishing of the interaction $U_{R^2}(\tilde{s}) = U_{R^2}(\tilde{s}^*) = 0$, whose functional form is defined in eq. (24). This means that, for tuning of the mass term to its critical value by an external field to be possible, the fluxes in each hexagonal lattice (hx, hx^*) ought to occur at the essential zeros of $\zeta(s)$ corresponding to $\text{Re}(s) = \Delta(d = 3) = 1/2$.

Finally, the argentophilic bonds described by eq. (1) and hence eq. (15) in the two-silver approximation ought to satisfy,

$$0 = 4J(\vec{r}_{ij})S_i^z S_j^z + \langle \langle h(\vec{r}_{ij}) \rangle \rangle (S_i^z + S_j^z), \quad (37)$$

where the double-averaging performed on $h(\vec{r}_{ij})$ given by eq. (20) corresponds to replacing \hat{s} and \hat{s}^* with their counterparts \tilde{s} and \tilde{s}^* respectively to yield,

$$\langle \langle h(\vec{r}_{ij}) \rangle \rangle = -\frac{m}{C} \left(\frac{\sqrt{2}a}{r_{ij}} \right)^{2(\tilde{s} + \tilde{s}^*)} = -\frac{Gm}{r_{ij}^2}, \quad (38)$$

with $\vec{r}_{ij} \in R^3$ strictly in R^3 , $\tilde{s} + \tilde{s}^* = 1$ from eq. (36), $G = 2a^2/C$ the square of the lattice constant with dimensions of [length]² and $J(\vec{r}_{ij}) = -A^2\chi_{\Delta(d)}(\vec{r}_{ij})$ the so-called Ruderman-Kittel-Kasuya-Yosida (RKKY) exchange interaction term in d dimensions (Fourier transform of the Lindhard function in d dimensions) characteristic of spin-orbit scattering of conduction electrons by the nonmagnetic (herein, pseudo-spin) impurities in calculations involving sd hybridisation[32] and,

$$\chi_{\Delta}(\vec{r}_{ij}) = -\frac{1}{4\pi} \left(\frac{m_{\Delta} k_F^2}{2\Delta + 1} \right) \left(\frac{k_F}{2\pi r_{ij}} \right)^{2\Delta} f_{\Delta}(k_F r_{ij}),$$

$$f_{\Delta}(x) = \mathcal{J}_{\Delta(d)}(x)\mathcal{Y}_{\Delta(d)}(x) + \mathcal{J}_{\Delta(d)+1}(x)\mathcal{Y}_{\Delta(d)+1}(x).$$

Here, $m_{\Delta(d)}$ is the generated electron mass on the honeycomb lattice due to bifurcation, A^2 a proportionality constant and $\mathcal{J}_{\alpha}(x), \mathcal{Y}_{\alpha}(x)$ are Bessel functions of the first and second kind respectively. Since $\chi_{\Delta}(\vec{r}_{ij})$ is proportional to the generated mass, $m_{\Delta(d)} = 2m\Delta(d)$, evidently $J(\vec{r}_{ij})$ is finite only in $d = 3$, allowing its positive value to counteract the $\vec{r}_{ij} \notin R^2$ pseudo-spin term in eq. (15) thus obtaining $H = 3J(\vec{r}_{ij}) + h(\vec{r}_{ij}) = 0$ as the final result of the calculations that commenced from eq. (1). In $d = 3$ dimensions (3D), where the RKKY terms are finite,

$$\begin{aligned} \chi_{\Delta(3)}(r_{ij}) &= \frac{mk_F}{8\pi^3 r_{ij}^3} \left(\frac{\sin(2k_F r_{ij})}{2k_F r_{ij}} - \cos(2k_F r_{ij}) \right) \\ &= -mk_F/8\pi^3 r_{ij}^3, \end{aligned} \quad (40)$$

where the last line is obtained by the constraints $\vec{r}_{ij} \cdot \vec{k}_{ij} = \pi N \neq 0$ and $\vec{r}_{ij} \times \vec{k}_{ij} = \vec{0}$. Here, $N \in \mathbb{N}$ is a non-vanishing positive integer, $\vec{r}_{ij} \neq 0, \vec{k}_{ij} \neq 0$ are both vectors in R^3 , $|\vec{r}_{ij}| = r_{ij}$ and $|\vec{k}_{ij}| = k_F$ defines the Fermi surface.

The final expression for the argentophilic bond becomes,

$$0 = \frac{L^2}{m^2 r_{ij}^3} - \frac{Gm}{r_{ij}^2} \equiv -\frac{\partial V(\vec{r}_{ij})}{\partial r_{ij}}, \quad (41a)$$

where,

$$V(\vec{r}_{ij}) = \frac{1}{2m^2} \frac{L^2}{r_{ij}^2} - \frac{Gm}{r_{ij}^2}, \quad (41b)$$

is the bonding potential and we have introduced $A^2 \equiv 8\pi^3 L^2 / 3k_F m^3$ in order to write the interaction in a familiar form, analogous to gravitational orbits under the potential $V(\vec{r}_{ij})$ representing the emergent attractive forces experienced by conduction electrons and diffusing silver cations in the material under a ‘Newton’s inverse-square law’ force with G playing the role of a ‘gravitational constant’ and L the angular momentum, leading to a conductor-semiconductor-insulator phase transition for all charge transport on the bifurcated lattice. The argentophilic bond length corresponds to $r_{\text{bond}} = L^2/Gm^3 \leq$

2.83 Å, which displays the relation between the constants L , m and G in terms of the observed bond length. However, since these constants are presently undetermined, for illustration purposes we shall set $r_{\text{bond}} \equiv 2.8$ Å and plot in Figure 6 the appropriately normalised potential,

$$V_{\text{bond}}^{(\tilde{m}^z, \tilde{c}^z)}(r_{ij}) = 2\tilde{c}^z r_{\text{bond}}^2 / 3r_{ij}^2 - \tilde{m}^z r_{\text{bond}} / r_{ij}, \quad (42)$$

for various values of $\Sigma_{ij} = (\tilde{m}^z, \tilde{c})$ in eq. (2), thus illustrating the presence of a minimum at r_{bond} only for the pseudo-spin wave function $\Sigma_{ij} = (+1, +3/4)_{ij}$ given in eq. (2). Changing the sign of the pseudo-magnetic field $h(\vec{r}_{ij}) \rightarrow -h(\vec{r}_{ij})$ exchanges pseudo-spin up with pseudo-spin down in the calculation in eq. (15), thus selecting instead $\Sigma_{ij} = (-1, +3/4)_{ij}$ as the potential with the minimum at r_{bond} .

Conclusion.—Exploiting the pseudo-spin degree of freedom in the bipartite honeycomb lattice of Ag cations inherited from the spin of their half-filled $4d_{z^2}$ orbitals, we introduced a pseudo-spin Heisenberg Hamiltonian to describe the argentophilic bond observed in silver-based bilayered materials, arriving at the same qualitative results as a previously proposed $\text{SU}(2) \times \text{U}(1)$ model.[1] In the Heisenberg Hamiltonian, the monolayer-bilayer phase transition occurs due to the spontaneous emergence of a pseudo-magnetic interaction term, with the mechanism for Ag bilayers reminiscent of Zeeman splitting. The advantage conferred by the proposed approach is the novel possibility of engineering a crossover between 2D and 3D behaviour of silver ions and their valence electrons expected to be responsible for particle pairing/bonding and a metal-semiconductor-insulator phase transition. Incidentally, since excellent conductors such as elemental silver are expected to be poor BCS superconductors due to fairly weak electron-phonon coupling[22], the electron pairing mechanism herein incidentally explains the low temperature superconductivity reported in $\text{Ag}_2^{1/2+}\text{F}$, *albeit* remains a normal conductor instead of semi-conductor or insulator[33] at temperatures well-above the reported transition temperature ($T_c \simeq 66$ mK).[34] Moreover, the silver bilayer in such materials is expected to be tuned not only by pseudo-magnetic fields in the form of stress and strain, but more readily by external magnetic fields whose flux values occur at the essential zeros of the so-called $L(s)$ functions such as the famous Riemann zeta function, corresponding to the Mellin transform of specific lattice theta functions.[12, 29] Such experiments should be performed on (near-)single crystals of pure silver-bilayered materials such as $\text{Ag}_2^{1/2+}\text{F}$ or the more stable $\text{Ag}_6^{1/2+}\text{Mg}_2\text{TeO}_6$ (or preferably any other silver bilayered material with non-magnetic slab cations in order to avoid effects such as magneto-resistance[35] due to magnetic ordering of $M = \text{Ni, Co, Cu}$ *etc* cations in the slabs) prepared, for instance, by mechanical exfoliation.[35]

Acknowledgements.—This work was supported in part

by the AIST Edge Runners Funding and Iketani Science and Technology Foundation.

* gmkanyolo@mail.uec.jp; gm.kanyolo@aist.go.jp
† titus.masese@aist.go.jp

- [1] T. Masese, G. M. Kanyolo, Y. Miyazaki, M. Ito, N. Taguchi, J. Rizell, S. Tachibana, K. Tada, Z.-D. Huang, A. Alshehabi, *et al.*, Honeycomb layered oxides with silver atom bilayers and emergence of non-abelian $\text{SU}(2)$ interactions, *Advanced Science*, 2204672 (2022).
- [2] D. Kurzydłowski, M. Derzsi, E. Zurek, and W. Grochala, Fluorides of silver under large compression, *Chemistry—A European Journal* **27**, 5536 (2021).
- [3] A. Grzelak, J. Gawraczyński, T. Jaroń, D. Kurzydłowski, Z. Mazej, P. Leszczyński, V. Prakapenka, M. Derzsi, V. Struzhkin, and W. Grochala, Metal fluoride nanotubes featuring square-planar building blocks in a high-pressure polymorph of AgF_2 , *Dalton Transactions* **46**, 14742 (2017).
- [4] H. Schneider, A. D. Boese, and J. M. Weber, Unusual hydrogen bonding behavior in binary complexes of coinage metal anions with water, *The Journal of chemical physics* **123**, 084307 (2005).
- [5] S. J. Dixon-Warren, R. Gunion, and W. Lineberger, Photoelectron spectroscopy of mixed metal cluster anions: NiCu^- , NiAg^- , NiAg_2^- , and Ni_2Ag^- , *The Journal of chemical physics* **104**, 4902 (1996).
- [6] J. Ho, K. M. Ervin, and W. Lineberger, Photoelectron spectroscopy of metal cluster anions: Cu_n^- , Ag_n^- , and Au_n^- , *The Journal of chemical physics* **93**, 6987 (1990).
- [7] K. Minamikawa, S. Sarugaku, M. Arakawa, and A. Terasaki, Electron counting in cationic and anionic silver clusters doped with a $3d$ transition-metal atom: endo-vs. exohedral geometry, *Physical Chemistry Chemical Physics* **24**, 1447 (2022); Correction: Electron counting in cationic and anionic silver clusters doped with a $3d$ transition-metal atom: endo-vs. exohedral geometry, *Physical Chemistry Chemical Physics* **24**, 2664 (2022).
- [8] S.-H. Lee, H.-J. Chung, J. Heo, H. Yang, J. Shin, U.-I. Chung, and S. Seo, Band gap opening by two-dimensional manifestation of Peierls instability in graphene, *ACS Nano* **5**, 2964 (2011).
- [9] R. E. Peierls and R. Peierls, *Surprises in theoretical physics*, Vol. 10 (Princeton University Press, 1979).
- [10] M. Garcia-Bach, P. Blaise, and J.-P. Malrieu, Dimerization of polyacetylene treated as a spin-peierls distortion of the Heisenberg hamiltonian, *Physical Review B* **46**, 15645 (1992).
- [11] G. M. Kanyolo, T. Masese, A. Alshehabi, and Z.-D. Huang, Advances in honeycomb layered oxides: Part I—syntheses and characterisations of pnictogen- and chalcogen-based honeycomb layered oxides, preprint [10.48550/arXiv.2207.06499](https://arxiv.org/abs/2207.06499) (2022).
- [12] G. M. Kanyolo and T. Masese, Advances in honeycomb layered oxides: Part II—theoretical advances in the characterisation of honeycomb layered oxides with optimised lattices of cations, preprint [10.48550/arXiv.2202.10323](https://arxiv.org/abs/2202.10323) (2022).
- [13] A. Kovalevskiy, C. Yin, J. Nuss, U. Wedig, and M. Jansen, Uncommon structural and bonding proper-

ties in $\text{Ag}_{16}\text{B}_4\text{O}_{10}$, *Chemical science* **11**, 962 (2020).

[14] A. Lobato, M. A. Salvadó, and J. M. Recio, Comment on “Uncommon structural and bonding properties in $\text{Ag}_{16}\text{B}_4\text{O}_{10}$ ” by A. kovalevskiy, C. Yin, J. Nuss, U. Wedig, and M. Jansen, *Chem. Sci.*, 2020, 11, 962, *Chemical science* **12**, 13588 (2021).

[15] C. Yin, U. Wedig, and M. Jansen, Reply to the “Comment on “Uncommon structural and bonding properties in $\text{Ag}_{16}\text{B}_4\text{O}_{10}$ ” by A. kovalevskiy, C. Yin, J. Nuss, U. Wedig, and M. Jansen, *Chem. Sci.*, 2020, 11, 962”, *Chemical Science* **12**, 13593 (2021).

[16] A. Georgi, P. Nemes-Incze, R. Carrillo-Bastos, D. Faria, S. Viola Kusminskiy, D. Zhai, M. Schneider, D. Subramiam, T. Mashoff, N. M. Freitag, *et al.*, Tuning the pseudospin polarization of graphene by a pseudomagnetic field, *Nano letters* **17**, 2240 (2017).

[17] M. Mecklenburg and B. Regan, Spin and the honeycomb lattice: lessons from graphene, *Physical Review Letters* **106**, 116803 (2011).

[18] M. J. Allen, V. C. Tung, and R. B. Kaner, Honeycomb carbon: a review of graphene, *Chemical Reviews* **110**, 132 (2010).

[19] A. G. Kvashnin, L. A. Chernozatonskii, B. I. Yakobson, and P. B. Sorokin, Phase diagram of quasi-two-dimensional carbon, from graphene to diamond, *Nano Letters* **14**, 676 (2014).

[20] M. Said, D. Maynau, J. P. Malrieu, and M. A. Garcia-Bach, A non-empirical Heisenberg Hamiltonian for the study of conjugated hydrocarbons. ground-state conformational studies, *Journal of the American Chemical Society* **106**, 571 (1984).

[21] J. J. Sakurai and E. D. Commins, Modern quantum mechanics, revised edition (1995).

[22] M. Tinkham, *Introduction to superconductivity* (Courier Corporation, 2004).

[23] R. D. Mattuck, *A guide to Feynman diagrams in the many-body problem* (Courier Corporation, 1992).

[24] G. M. Kanyolo and T. Masese, An idealised approach of geometry and topology to the diffusion of cations in honeycomb layered oxide frameworks, *Scientific Reports* **10**, 13284 (2020).

[25] G. M. Kanyolo and T. Masese, Cationic vacancies as defects in honeycomb lattices with modular symmetries, *Scientific Reports* **12**, 1 (2022).

[26] M. A. Pinsky, *Introduction to Fourier analysis and wavelets*, Vol. 102 (American Mathematical Soc., 2008).

[27] N. J. A. Sloane, *Theta series of planar hexagonal lattice \mathbf{A}_2* , The Online Encyclopedia of Integer Sequences (1964), accessed in June, 2023.

[28] X.-X. Liu, C. P. Oberndorfer, and M. Jansen, Electrochemical de-/intercalation of silver for Ag_2NiO_2 and AgNiO_2 , *Journal of The Electrochemical Society* **155**, E1 (2007).

[29] J. B. Conrey, The riemann hypothesis, *Notices of the AMS* **50**, 341 (2003).

[30] N. J. A. Sloane, Nearest integer to imaginary part of n -th zero of riemann zeta function, The Online Encyclopedia of Integer Sequences (1964), accessed in June, 2023.

[31] S.-D. Liang, Y.-H. Bai, and B. Beng, Peierls instability and persistent current in mesoscopic conducting polymer rings, *Physical Review B* **74**, 113304 (2006).

[32] D. Aristov, Indirect RKKY interaction in any dimensionality, *Physical Review B* **55**, 8064 (1997).

[33] X.-l. Wang and M. Ikezawa, Anisotropic drude reflectivity of Ag_2F crystal, *Journal of the Physical Society of Japan* **60**, 1398 (1991).

[34] K. Andres, N. Kuebler, and M. Robin, Superconductivity in Ag_2F , *Journal of Physics and Chemistry of Solids* **27**, 1747 (1966).

[35] H. Taniguchi, M. Watanabe, M. Tokuda, S. Suzuki, E. Imada, T. Ibe, T. Arakawa, H. Yoshida, H. Ishizuka, K. Kobayashi, *et al.*, Butterfly-shaped magnetoresistance in triangular-lattice antiferromagnet Ag_2CrO_2 , *Scientific Reports* **10**, 1 (2020).